ESR in CrCl3-based graphite intercalation and bi-intercalation compounds

S. Chehab, P. Biensan, J. Amiell, S. Flandrois

Classification
Physics Abstracts
76.30F

ESR in $CrCl_3$-based graphite intercalation and bi-intercalation compounds

S. Chehab, P. Biensan, J. Amiell and S. Flandrois

Centre de Recherche Paul Pascal, C.N.R.S., Château Brivazac, 33600 Pessac, France

(*Received 14 September 1990, revised 29 October 1990, accepted 13 December 1990*)

Abstract. — ESR experiments have been performed on stage-1, -2, -3, $CrCl_3$ graphite intercalation compounds as well as on $CrCl_3$-$CdCl_2$ and $CrCl_3$-$MnCl_2$ graphite bi-intercalation compounds. The measurements have been carried out at the X-band frequency and over the temperature range $4.2\ K \leq T \leq 294\ K$. The variation of the linewidth (ΔH) and the resonance field (H_r) have been examined as a function of the temperature and the angle θ between the external field and the crystal *c*-axis. The results reflect the anisotropic 2D character of these systems. The room temperature angular dependence of ΔH follows a $(3\cos^2\theta - 1)^2$-like behavior and that of H_r has a $(3\cos^2\theta - 1)$-like form. For the singly intercalated systems, ΔH decreases with T according to $(1 - \Theta_{cw}/T)$ in the high temperature region, then shows a local minimum at around 35 K followed by a critical-like divergence at lower temperatures. In the bi-intercalated compounds, ΔH *vs.* T exhibits three types of behavior : for $T \geq 220$ K, ΔH behaves like T^2; for $120\ K \leq T \leq 220\ K$ ΔH seems to be proportional to $(1 - \Theta_{cw}/T)$; for $T \leq 120$ K, ΔH shows a gradual increase which becomes steeper and steeper with falling T. The T^2-like behavior may be explained in connection to a spin-lattice relaxation phenomenon which becomes important at high temperatures. The temperature dependence of H_r is characterized by an increase of $H_{r\parallel}$ and a decrease of $H_{r\perp}$ with decreasing temperature. This is consistent with the theoretical predictions developed for anisotropic low-dimensional systems, reflecting the increase in the anisotropy of low temperature susceptibility.

1. Introduction.

Graphite intercalation compounds (GIC's) with magnetic species as intercalants, have generated considerable interest in the study of 2D magnetism [1, 2]. The advantage that this class of materials presents is the possibility of controlling the magnetic dimensionality by varying the number of carbon layers i.e. the stage number, between the magnetic planes. In this respect, a considerable amount of work has been carried out on various transition metal chloride GIC's, mainly $CoCl_2$-, $NiCl_2$- and $MnCl_2$-GIC's [3-5]. The in-plane structure and magnetic interactions of the intercalants are nearly the same as those of their pristine form. At the same time, the interplanar repeat distance is greatly increased by the presence of intervening graphite layers, leading in turn to a dramatic reduction in the interlayer magnetic

coupling. These compounds have been found to exhibit low temperature magnetic phase transitions the nature of which has yet to be fully understood [6, 7].

Recently, more complicated systems, known as graphite bi-intercalation compounds (GBIC's), have been synthesized and studied [8]. These systems contain a regular sequence of two kinds of intercalated layers which can be both magnetic, e.g. $FeCl_3$-$NiCl_3$-GBIC, or one magnetic and the other non-magnetic, e.g. $CrCl_3$-$AlCl_3$-GBIC. While the former case offers the possibility of studying the interaction between the two types of magnetic guests, the latter allows greater separation between the magnetic planes relative to that in the associated simpler GIC's. This, certainly, leads to enhanced bidimensionality, the effect of which on the magnetic behavior can be explored.

Pristine $CrCl_3$ has a hexagonal layered type crystal structure. It undergoes a magnetic phase transition below $T = 16.8$ K to an antiferromagnetic state, with the spins lying in the basal planes and forming ferromagnetic layers which alternate in direction along the c-axis [9]. The paramagnetic state is characterized by a positive Curie-Weiss temperature near 29 K, and the ordered state by a strong field-dependent susceptibility. This magnetic behavior is explained by a strong ferromagnetic coupling within each layer, and a relatively weak antiferromagnetic coupling between adjacent layers that can be disturbed in relatively weak external fields. The above described characteristics of $CrCl_3$ are very similar to those of $CoCl_2$ and $NiCl_2$ [10]. However, very little work relating to $CrCl_3$-GIC's is found in the literature, very likely because of the difficulty with which the intercalation process of $CrCl_3$ in graphite occurs [11].

Members of our group have recently synthesized and characterized new compounds of stage-1, -2 and -3 $CrCl_3$-GIC's, as well as $CrCl_3$-$CdCl_2$- and $CrCl_3$-$MnCl_2$-GBIC's. Preliminary investigations of their magnetic properties by ac susceptibility and magnetization measurements have revealed a transition temperature, T_c, around 11 K [12, 13]. Below T_c, a large hysterisis behavior is exhibited between the zero-field-cooled and field-cooled magnetizations, as in the case of $CoCl_2$- and $NiCl_2$-GIC's. In the present work, the magnetic properties of these compounds are investigated by ESR experiments. The angular and temperature dependence of the linewidth and resonance field are discussed in connection with the spin dynamics in 2D magnetic systems.

2. Experimental procedures.

The stage-3 $CrCl_3$-GIC samples were prepared from single crystals of Madagascar natural graphite by vapor reaction of $CrCl_3$ in a chlorine atmosphere ($T = 800$ °C, $P_{Cl} = 4$ atm.). The preparation of stage-1 and -2 $CrCl_3$-GIC's was possible only with Kish graphite ($\varphi = 3$ mm), under the same reaction conditions as above. For the synthesis of the bi-intercalation compounds, $CrCl_3$-$CdCl_2$- and $CrCl_3$-$MnCl_2$-GBIC's, the synthesized stage-3 $CrCl_3$-GIC (in which two graphite interlayers out of three remain unoccupied) was used as a starting material. This was made possible because of the very high intercalation temperature (800 °C) of $CrCl_3$. The stage-3 $CrCl_3$-GIC was thus heated in the presence of $CdCl_2$, or $MnCl_2$, under the same reaction conditions that are required for the preparation of stage-1 $CdCl_2$-GIC, or $MnCl_2$-GIC. The so produced materials are of stage-1 GBIC's with intercalate stacking sequence A/B/B/A where A = $CrCl_3$ and B = $CdCl_2$ or $MnCl_2$, / = graphite layer. All the synthesized samples were structurally characterized by (00 L) and precession X-ray diffraction techniques, revealing that, after intercalation, both the chloride layers and the graphite layers have kept the same crystallographic aspects as those found in the corresponding pristine materials. Further details on materials synthesis and characterization are reported elsewhere [14].

The ESR measurements were performed at X-band using a field-modulated spectrometer,

in the temperature range between 4.2 and 294 K. The magnetic field was rotated in a plane containing the c-axis and perpendicular to the c-plane.

3. Results, analysis and discussion.

3.1 GENERAL FEATURES OF THE ESR LINESHAPE. — For all the investigated systems, a single Dysonian ESR line is observed (see Fig. 1) down to about 18 K. The asymmetry ratio A/B is found to lie approximately between 2 and 4, lower than for pure graphite ($A/B \approx 6$). Below 18 K, the ESR spectrum becomes complex and consists of at least two, and up to five, resonance lines, depending on the crystal considered and on its orientation with respect to the applied magnetic field. Similar types of behavior have also been observed in the cases of $NiCl_2$-GIC [15, 16] and Eu-GIC [21], the origin of which has not yet been fully or satisfactorily interpreted.

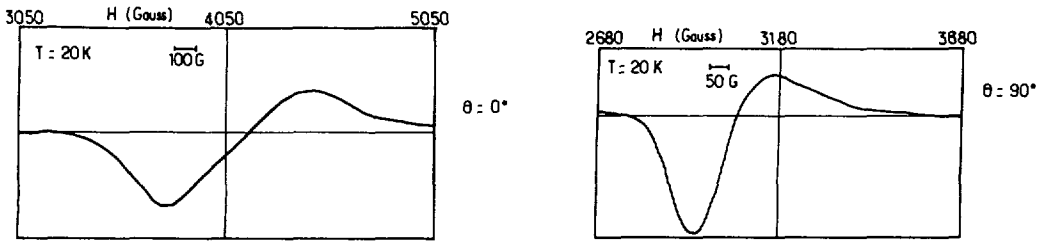

Fig. 1. — Example of ESR lineshape for both orientations $H_{ap} // C$ ($\theta = 0°$) and $H_{ap} \perp C$ ($\theta = 90°$). This represents the case of $CrCl_3$-$CdCl_2$-GBIC at $T = 20$ K.

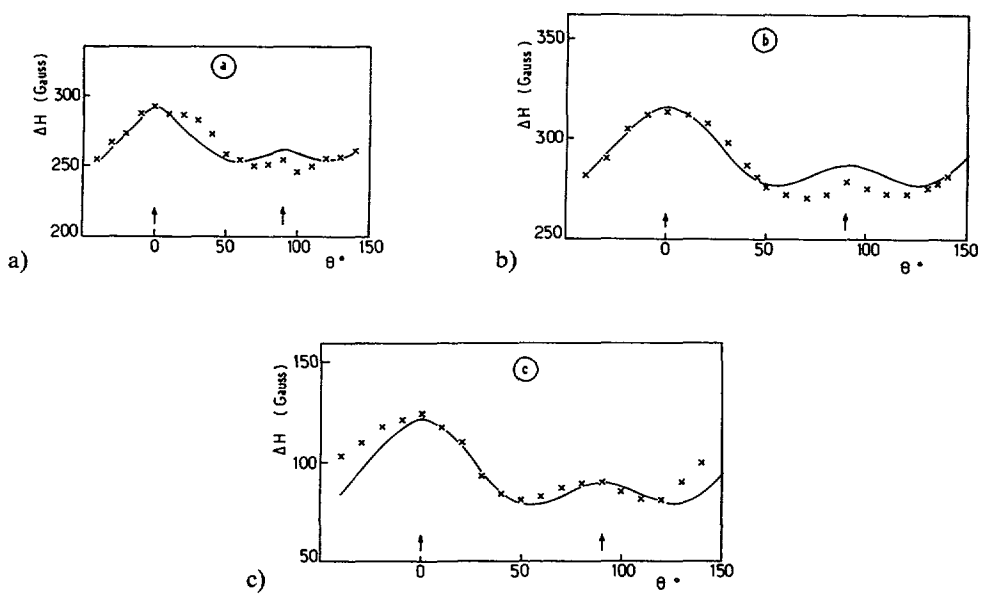

Fig. 2. — Angular dependence of the linewidth at room temperature for (a) stage-1 $CrCl_3$-GIC ; (×) experimental data, (——) fitted curve $\Delta H(\theta) = 9.5\,(3\cos^2\theta - 1)^2 + 275$; (b) stage-3 $CrCl_3$-GIC ; (×) experimental data, (——) fitted curve $\Delta H(\theta) = 9.8\,(3\cos^2\theta - 1)^2 + 277$; (c) $CrCl_3$-$CdCl_2$-GBIC ; (×) experimental data, (——) fitted curve $\Delta H(\theta) = 11\,(3\cos^2\theta - 1)^2 + 78$.

3.2 ANGULAR DEPENDENCE OF THE LINEWIDTH. — The variation of the linewidth, at room temperature, as a function of the angle θ formed between the c-axis and the external applied field H_{ap}, for stage-1 and -3 $CrCl_3$-GIC and for $CrCl_3$-$CdCl_2$-GBIC, is shown in figures 2a, 2c. The data follow the general form of the function :

$$\Delta H = A\,(3\cos^2\theta - 1)^2 + B\,. \tag{1}$$

Similar behavior has been observed in other pseudo-bidimensional (both Ferro and Antiferro) magnetic systems, such as K_2CuF_4 [22], K_2MnF_4 [23], $NiCl_2$-GIC [15-17] and $MnCl_2$-GIC's (stages 1 and 2) [17-19]. It is characterized by two maxima in ΔH at around $\theta = 0°$ and $\theta = 90°$, with the former being larger than the latter, also by a local minimum at θ around 55°. As shown by Richards *et al.* [23, 24], this behavior is characteristic of 2D Heisenberg magnetic systems (with 2D dipolar and isotropic exchange interactions [34]), and arises from the dominant role of the $q \to 0$ modes in the long-time decay of the spin correlation function in these systems.

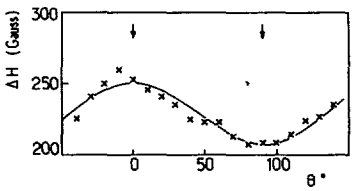

Fig. 3. — Angular dependence of the linewidth at room temperature for $CrCl_3$-$MnCl_2$-GBIC ; (×) experimental data, (——) fitted curve $\Delta H(\theta) = 42\cos^2\theta + 208$.

The angular dependence of the linewidth in the case of the bi-intercalation compound $CrCl_3$-$MnCl_2$, as shown in figure 3, can not be described by equation (1), but rather appears to have a $\cos^2\theta$-like form, with no minimum around $\theta = 55°$, However, this compound, unlike the rest, contains two different magnetic species, Mn and Cr, both of which are ESR active. The observed ESR signal should thus represent the average response of both systems. Considering that the ΔH *vs.* θ behavior of the singly intercalated compounds of $MnCl_2$ and of $CrCl_3$ follows equation (1) closely, it is a little surprising to find that this is not the case in the bi-intercalation compound. Nevertheless, the important aspect of the 2D behavior, that the linewidth ΔH at $\theta = 0°$ is larger than that at $\theta = 90°$, is respected.

3.3 ANGULAR DEPENDENCE OF THE RESONANCE FIELD. — The room temperature g-values for $H_{ap} \,/\!/\, c\,(g_\parallel)$ and $H_{ap} \perp c\,(g_\perp)$ are listed in table I, for all the investigated compounds.

Table I. — *$g_\parallel$ and $g_\perp$ values at room temperature. The notations // and ⊥ refer to H_{ap} parallel and perpendicular to the c-axis respectively.*

Compound	$g_\parallel$	$g_\perp$	
$CrCl_3$ (Pure)	1.984	1.989	Ref. [25]
stage-1 $CrCl_3$-GIC	1.981	1.993	
stage-2 $CrCl_3$-GIC	1.978	1.986	
stage-3 $CrCl_3$-GIC	1.976	1.983	
$CrCl_3$-$CdCl_2$-GBIC	1.988	1.992	
$CrCl_3$-$MnCl_2$-GBIC	1.974	1.978	

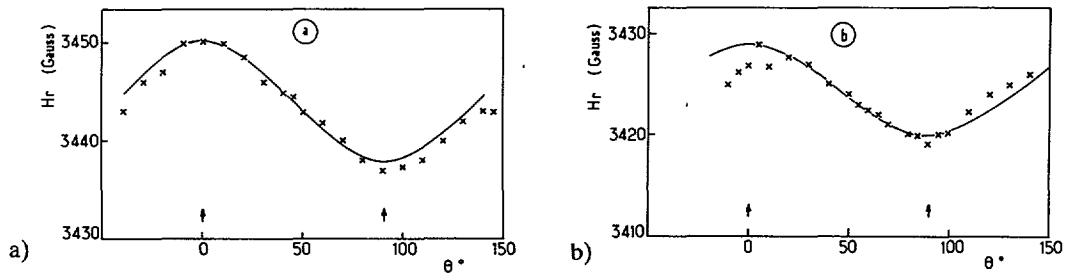

Fig. 4. — Angular dependence of the resonance field at room temperature ; ν = 9.54 GHz (a) stage-3 $CrCl_3$-GIC ; (×) experimental data, (——) fitted curve $H_r(\theta) = 4(3\cos^2\theta - 1) + 3\,442$; (b) $CrCl_3$-$CdCl_2$-GBIC ; (×) experimental data, (——) fitted curve $H_r(\theta) = 3(3\cos^2\theta - 1) + 3\,423$.

These values are very close to those of Cr^{3+} in pure $CrCl_3$ [25], also listed for comparison. The angular dependence of the resonance field H_r for $CrCl_3$-GIC and $CrCl_3$-$CdCl_2$-GBIC is shown in figures 4a, 4b. The data of H_r *vs.* θ seems to be well described by the general form of the function :

$$H_r = C(3\cos^2\theta - 1) + D\,. \tag{2}$$

This form of angular anisotropy has been explained by the non-cubic distribution of dipoles in the 2D lattice [15, 22]. The resulting net dipolar field shifts the resonance field according to equation (2). This behavior has been also observed in K_2MnF_4 [22], $NiCl_2$-GIC [15-17] and $MnCl_2$-GIC [17-19].

As in the case of its linewidth behavior, $CrCl_3$-$MnCl_2$-GBIC shows an anomalistic H_r *vs.* θ dependence. As seen from figure 5, an extra maximum is displayed in the region between 50° and 60°. The origin of this compound's unusual behavior is not quite clear at the present time : further experimental investigations are required before a final conclusion can be drawn.

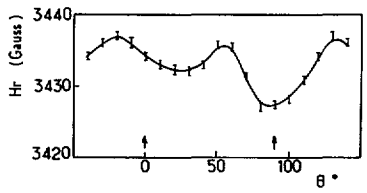

Fig. 5. — Angular dependence of the resonance field at room temperature for $CrCl_3$-$MnCl_2$-GBIC (——) guide for the eye ; ν = 9.49 GHz.

3.4 TEMPERATURE DEPENDENCE OF THE LINEWIDTH. — The variation of the linewidth ΔH with temperature T for stage-1 and -3 $CrCl_3$-GIC's are plotted in figures 6 and 7, for both directions of H_{ap} parallel and perpendicular to the c-axis. As T is decreased from room temperature, ΔH decreases continuously and, after reaching a minimum at about 35 K, it increases divergently. According to the theoretical predictions of Richards [24], the linewidth of 2D magnetic system can be expressed, in the high-temperature limit, by :

$$\Delta H = (1 - \Theta_{cw}/T)\,\Delta H_\infty \tag{3}$$

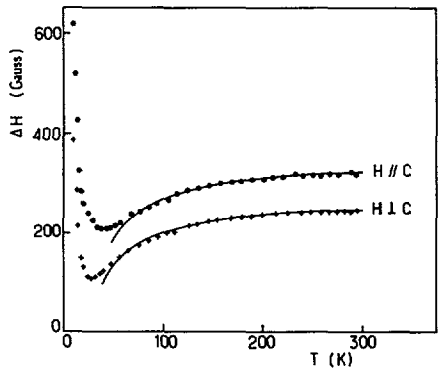

Fig. 6. — Temperature dependence of the linewidth for stage-1 $CrCl_3$-GIC ; (•) $H_{ap}/\!/C$ ($\theta = 0°$), (+) $H_{ap} \perp C$ ($\theta = 90°$). The solid lines represent the calculated curves of equation (3) using the proper values for the parameters Θ_{cw} and ΔH_∞ listed in table II.

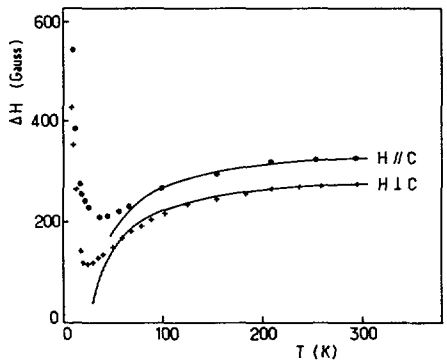

Fig. 7. — Temperature dependence of the linewidth for stage-3 $CrCl_3$-GIC ; (•) $H_{ap}/\!/C$ ($\theta = 0°$), (+) $H_{ap} \perp C$ ($\theta = 90°$). The solid lines represent the calculated curves of equation (3) using the proper values for the parameters Θ_{cw} and ΔH_∞ listed in table II.

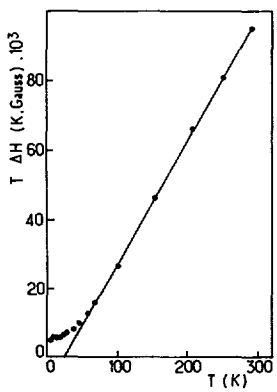

Fig. 8. — Typical plot of $T\,\Delta H$ *vs.* T for the case of singly intercalated compounds. The data shown here are for stage-3 $CrCl_3$-GIC, $H_{ap}/\!/C$. Values of the parameters Θ_{cw} and ΔH_∞ of equation (3) are obtained from the slope and intercept of the linear part of the plot.

where Θ_{cw} is the Curie-Weiss paramagnetic temperature found in the magnetic susceptibility behavior, and ΔH_∞ is the linewidth at infinite temperature. If this was the case then a plot of $T\,\Delta H$ against T in the high-temperature region should yield a straight line behavior, since equation (3) can be written as $T\,\Delta H = (T - \Theta_{cw})\,\Delta H_\infty$. This is indeed observed for both compounds (stages 1 and 3) and for both orientations (// and ⊥); also, as illustrated in figure 8, which shows a typical example of a $T\,\Delta H$ *vs.* T plot, this linear behavior is observed down to just above 50 °K. The values of ΔH_∞ and Θ_{cw} for each case, which can be obtained from the slope and the intercept of the straight line, are listed in table II. Using these values in equation (3), ΔH *vs.* T curves are calculated and compared with the experimental data in figures 5 and 6. The excellent agreement between the experimental points and the calculated curves is evident and persists down to at least 60 K. It is important to note that the values of

Table II. — *Values of equation* (1) *parameters* Θ_{cw} *and* ΔH_∞. *The notations // and ⊥ refer to* H_{ap} *parallel and perpendicular to the c-axis respectively.*

Compound	$\Theta_{cw\parallel}$ (K)	$\Delta H_{\infty\parallel}$ (Gauss)	$\Theta_{cw\perp}$ (K)	$\Delta H_{\infty\perp}$ (Gauss)
stage-1 $CrCl_3$-GIC	24	355	25	270
stage-3 $CrCl_3$-GIC	25	355	26	300
$CrCl_3$-$CdCl_2$-GBIC	20	110	22	69
$CrCl_3$-$MnCl_2$-GBIC	27	200	28	121

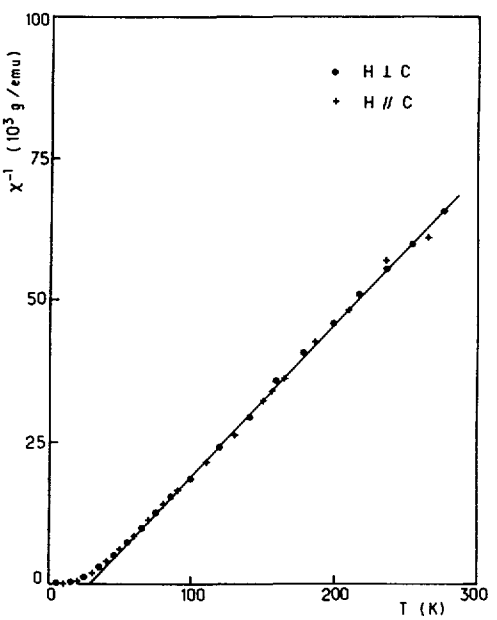

Fig. 9. — Typical variation of the inverse magnetic susceptibility with temperature. This plot represents the case of stage-3 $CrCl_3$-GIC for both applied field orientations: (•) $H_{ap}//C$ and (+) $H_{ap} \perp C$, H_{ap} = 1 000 Gauss.

Θ_{cw} deduced from this analysis are in excellent agreement with those obtained from magnetic susceptibility measurements carried out on these compounds [14] (as illustrated in Fig. 9), which in turn are very close to $\Theta_{cw} = 29$ K of pure $CrCl_3$ (R). Suzuki *et al.* have observed similar behavior in 2nd-stage $NiCl_2$-GIC based on HOPG graphite [15, 16].

As indicated above, further lowering of temperature below 35 K leads to a divergent increase in the linewidth ΔH. Such a behavior is characteristic of pretransitional spin fluctuation. Indeed, based on theoretical considerations, Richards [24] has demonstrated that, for 2D ferromagnetic systems, the $q \to 0$ modes of spin fluctuation grow in strength as the temperature is lowered toward the critical temperature, leading to the observed divergence in ΔH.

The variations of the linewidth with temperature for $CrCl_3$-$CdCl_2$-GBIC and for $CrCl_3$-$MnCl_2$-GBIC, are shown in figures 10 and 11. As seen, the ΔH *vs.* T data for both bi-intercalated compounds have the same general behavior which is different from that of $CrCl_3$-GIC's, mainly in the high temperature region. As the temperature is lowered from room temperature, the linewidth decreases at a relatively fast rate until about 220 K ; from this point, down to about 100 K, the decrease in ΔH occurs at a much slower rate. Below 100 K, ΔH exhibits a small but gradual increase, becoming steeper and steeper with further decreasing temperature. The plots of $T\,\Delta H$ *vs.* T, a typical example of which is presented in figure 12, show that the linear behavior is respected only in the temperature region between approximately 100 K and 220 K. The values of the parameters ΔH_∞ and Θ_{cw} obtained from the linear region are listed in table II. Again the values of Θ_{cw} are in close agreement with those obtained from magnetic susceptibility measurements. As demonstrated in figures 10 and 11, for temperatures higher than about 220 K, the measured linewidth values quickly rise above the calculated ΔH *vs.* T curves obtained from equation (3). We point out that, as has

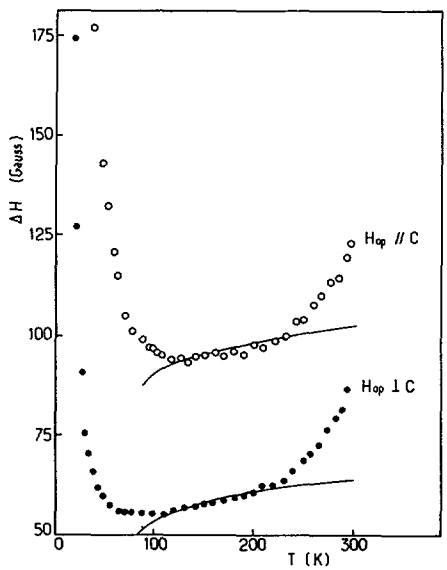

Fig. 10. — Temperature dependence of the linewidth for $CrCl_3$-$CdCl_2$-GBIC ; (O) $H_{ap}/\!/C$ ($\theta = 0°$), (•) $H_{ap} \perp C$ ($\theta = 90°$). The solid lines represent the calculated curves of equation (3) using the proper values for the parameters Θ_{cw} and ΔH_∞ listed in table II.

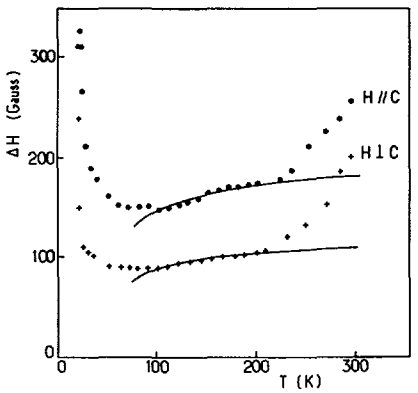

Fig. 11. — Temperature dependence of the linewidth for $CrCl_3$-$MnCl_2$-GBIC ; (•) $H_{ap}//C$ ($\theta = 0°$), (+) $H_{ap} \perp C$ ($\theta = 90°$). The solid lines represent the calculated curves of equation (3) using the proper values for the parameters Θ_{cw} and ΔH_{∞} listed in table II.

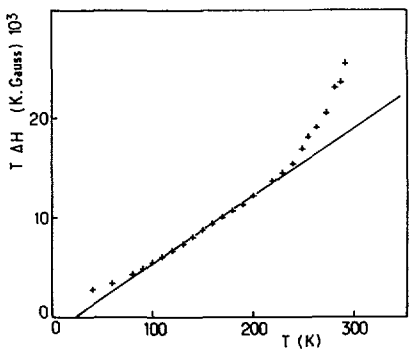

Fig. 12. — Typical plot of $T\,\Delta H$ *vs.* T for the case of doubly intercalated compounds. The data shown here are for $CrCl_3$-$CdCl_2$-GBIC, $H_{ap} \perp C$. Values of the parameters Θ_{cw} and ΔH_{∞} of equation (3) are obtained from the slope and intercept of the linear part of the plot.

been observed by Brown [26], pristine $CrCl_3$ exhibits a similar fast rise in its ESR linewidth behavior but starting at a much higher temperature of about 513 K. Interpolating between the pristine $CrCl_3$ and the $CrCl_3$-based bi-intercalation compounds, we expect the ΔH *vs.* T behavior in $CrCl_3$-GIC's to show a similar rise at a temperature somewhere above 294 K (our highest measurement temperature) but below that of pure $CrCl_3$.

It has been shown by Huber *et al.* [27], Richards [24] and Jaccarino *et al.* [28] that, in concentrated magnetic systems, the ESR linewidth should approach a temperature independent value (ΔH_{∞} in Eq. (3)) in the high temperature limit, provided that there is no contribution to ΔH from sources other than the magnetic ions spin-spin interactions. However, Huber *et al.* argue that in non S-state concentrated magnetic systems (i.e. orbital momentum of magnetic ions $\neq 0$) with spin $S \geqslant 1$, such as the magnetic compounds of Cr^{3+} and Ni^{2+}, the spin-lattice relaxation mechanism could have a significant contribution to ΔH which, consequently, would show a T-like or T^2-like behavior in the high temperature limit, depending on whether a one-phonon or two-phonon process is involved, respectively. This sort of behavior is clearly evidenced in the cases of pure $CrBr_3$ [27], $NiCl_2$ [29] and, as

mentioned above, in $CrCl_3$ [26]. In this context, the observed linewidth results from the contributions of both spin-spin and spin-lattice mechanisms i.e. $\Delta H = \Delta H_{s-s} + \Delta H_{s-l}$. Applying this notion to the linewidth data in figures 10 and 11, and approximating ΔH_{s-s} by the calculated curves of equation (3), ΔH_{s-l} can then be estimated from the difference between the measured linewidth values and the calculated ones, $\delta = \Delta H - \Delta H_{s-s}$. (Of course this analysis concerns the non-critical high-temperature region.) From the plots of δ as a function of T^2, an example of which is shown in figure 13, a linear relationship can be inferred. This indicates that the spin-lattice relaxation mechanism in the present systems takes place through the two-phonon process.

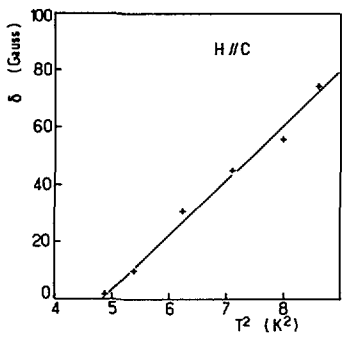

Fig. 13. — An example plot of $\delta = \Delta H_{exp} - \Delta H_{calc}$ as a function of T^2. The data shown here are for $CrCl_3$-$MnCl_2$-GBIC, $H_{ap} // C$.

Huber *et al.* [27] also discuss the angular dependence of the spin-lattice contribution to the linewidth ΔH_{s-l}. They argue that if the local symmetry of the ligands surrounding the magnetic ion is predominantly cubic, as is the case in the present compounds where the neighbouring chlorine ions are presumed to form a nearly perfect octahedron, then the spin-lattice relaxation rates along the three principal directions will be about the same. Consequently, we should have $(\Delta H_{s-l})_{\parallel} \approx (\Delta H_{s-l})_{\perp}$. This what is indeed observed here by comparing the δ values obtained from figures 10 and 11 for both orientations $H_{ap} // c$-axis and $H_{ap} \perp c$-axis.

3.5 TEMPERATURE DEPENDENCE OF THE RESONANCE FIELD. — The variations of the resonance field H_r with temperature are shown in figures 14a, 14d. For all investigated compounds, as T is decreased from room temperature, a gradual anisotropic shift in H_r is observed; $H_{r\parallel}(\theta = 0°)$ increases while $H_{r\perp}(\theta = 90°)$ decreases. This shift becomes stronger and stronger with temperature falling below 50 K. Such a behavior has already been observed for other uniaxially anisotropic 2D magnetic systems, namely K_2CuF_4 [30], K_2MnF_4 [31], $NiCl_2$-GIC [15-17, 20], $MnCl_2$-GIC [17-19] as well as Eu-GIC [21]. In this context, it has been theoretically shown first by Huber *et al.* [32] and then by Nagata *et al.* [31] that the anisotropic shift of H_r is directly related to the increase of anisotropy in the magnetic susceptibility with decreasing temperature (as illustrated in Figs. 15 and 16). This is understood to arise from the effects of the short-range ordering of spins and the anisotropy terms in the Hamiltonian. It follows from Huber's and Nagata's theories that the mean resonance field defined as:

$$H_{rm} = \{(H_{r\parallel}) \cdot (H_{r\perp})^2\}^{1/3},$$

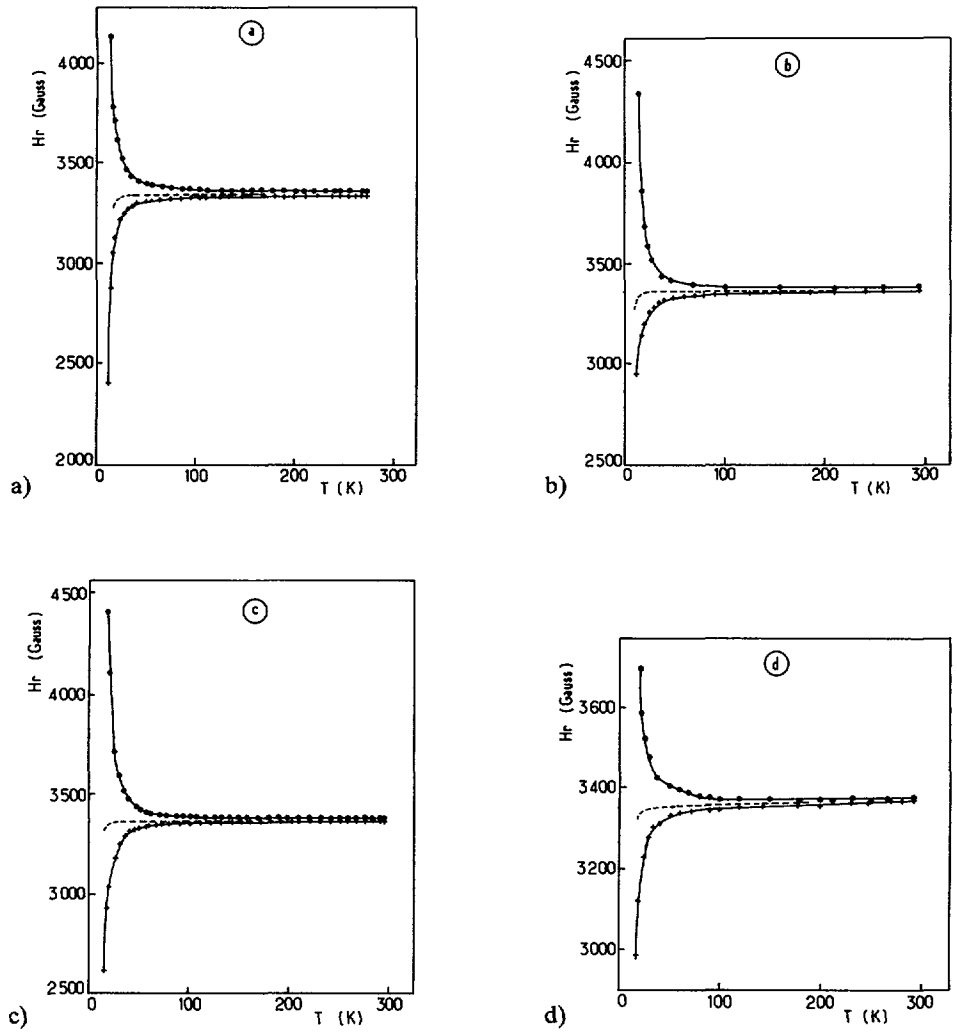

Fig. 14. — Temperature dependence of the resonance field ; $\nu = 9.35$ GHz. (•) $H_{ap}//C$ ($\theta = 0°$), (×) $H_{ap} \perp C$ ($\theta = 90°$). (——) guide for the eye, (-----) $H_{rm} = (H_{r\parallel} \times H_{r\perp}^2)^{1/3}$ (a) stage-1 $CrCl_3$-GIC ; (b) stage-3 $CrCl_3$-GIC ; (c) $CrCl_3$-$CdCl_2$-GBIC ; (d) $CrCl_3$-$MnCl_2$-GBIC.

should be independent of temperature for the Heisenberg system in the paramagnetic phase. As seen in figures 14, H_{rm} is found to be temperature independent down to a temperature T_g around 20 K to 24 K, depending on the compound, below which a downward deviation sets in. These results suggest that these compounds may be regarded as 2D ferromagnetic ([1]) systems with Heisenberg-like spin symmetry for T above T_g. It follows that there occurs a crossover of the spin symmetry from 2D Heisenberg-like to 2D XY-like at T around T_g. The XY spin symmetry in these compounds is believed to have the same origin as for pristine $CrCl_3$, where the easy-plane anisotropy field $H_{an}^{out} \sim 1$ kOe at 0 K [9]. This symmetry preserving field H_{an}^{out} decreases with increasing temperature and is expected to reduce to zero

([1]) Note that in the case of $MnCl_2$-$CrCl_3$-GBIC the $MnCl_2$ planes are expected to behave as 2D antiferromagnet.

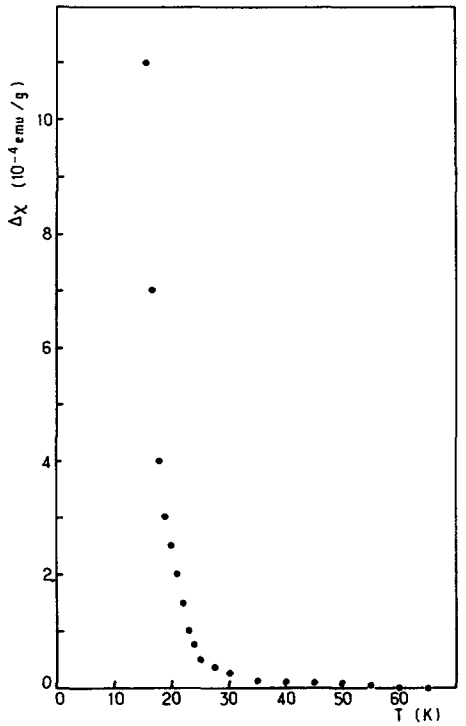

Fig. 15. — Representative variation of the susceptibility anisotropy $\Delta\chi = (\chi_\perp - \chi_\parallel)$ with temperature. The data are for the case of stage-3 $CrCl_3$-GIC. ($\perp$ and $/\!/$ mean the susceptibility for $H_{ap} \perp C$ and $H_{ap} /\!/ C$ respectively.) $H_{ap} = 1\,000$ Gauss.

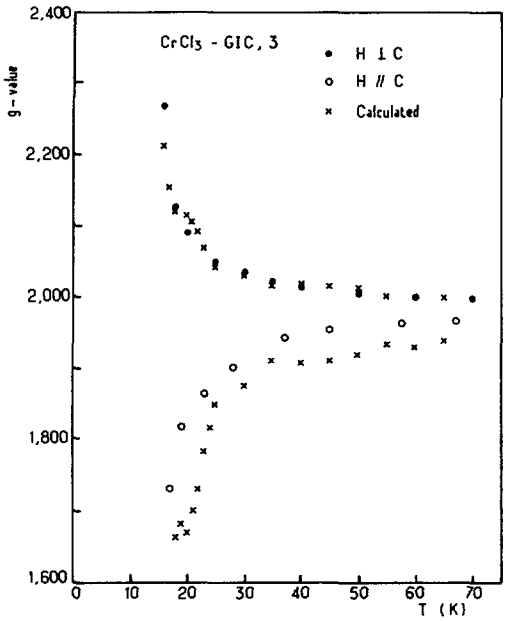

Fig. 16. — Comparison of the experimental g-shifts *vs.* T, obtained for $H_{ap} \perp C$ and $H_{ap} /\!/ C$, with those calculated from the theory of Nagata *et al.* [31] : $g_\parallel = g\,\{1 - \Delta\chi/\chi_\parallel\}$, $g_\perp = g\,\{1 + \Delta\chi/2\,\chi_\perp\}$. The data are for the case of stage-3 $CrCl_3$-GIC. The g-value = 1.980 is used in the calculation and is taken from table I. A qualitative agreement is evident.

at the crossover temperature which may coincides with T_g. The spin fluctuation is thus expected to have a 2D XY-like character for $T \leqslant T_g$, where $H_{an}^{out} \neq 0$, and a 2D Heisenberg-like character for $T \geqslant T_g$, where $H_{an}^{out} = 0$. Similar observations have been made in the case of $NiCl_2$-GIC by Suzuki *et al.* [16, 17], but a T_g value of the order of 30 K was found.

4. Conclusion.

The magnetic bidimensionality of $CrCl_3$-based graphite intercalated and biintercalated compounds is well revealed by our ESR investigations. In effect, the $(3 \cos^2 \theta - 1)^2$-like angular dependence observed for the linewidth ΔH and $(3 \cos^2 \theta - 1)$ for the resonance field H_r are characteristic for 2D magnetic systems [15, 23, 24]. The anisotropic shift of H_r with falling temperature underlines the uniaxial anisotropy associated with the 2D lattice [31, 32]. The $(1 - \Theta_{cw}/T)\ \Delta H_\infty$ behavior found for the linewidth in the high-temperature region and ΔH's subsequent divergence at low temperatures goes along with the 2D magnetic character [24]. In the case of the biintercalation compounds, it appears that, in addition to the spin-spin interaction which is responsible for the above mentioned ΔH *vs.* T behavior, there is a spin-phonon interaction effect which becomes important above 220 K, giving rise to a T^2-like dependence for ΔH. It is worth noting that the general similarity observed between most of the ESR aspects of both Cr-Cd and Cr-Mn biintercalated compounds, in association with the fact that Cd is non-magnetic, seem to suggest that, in the Cr-Mn compound, the Cr ions somehow play a more dominant role in the determination of the ESR response than the those of Mn.

As we know, the parameter which characterizes the magnetic bidimensionality is defined by the ratio of the intraplanar to the interplanar magnetic interaction, $r = Jz/J' z'$. In pristine $CrCl_3$, $r \approx 425$ [9] which is an order of magnitude larger than in $CoCl_2$ (≈ 13) and in $NiCl_2$ (≈ 20) [5, 33]. The introduction, between the consecutive $CrCl_3$ layers, of one, two or three carbon layers (as well as non-magnetic layers such as $CdCl_2$ in the biintercalation case) is known to enhance r by several orders of magnitude, as has been shown for $CoCl_2$- and $NiCl_2$-GIC's [1-5]. Consequently, $CrCl_3$-based intercalation and biintercalation compounds are expected to constitute excellent systems for the study of 2D magnetism.

Finally, the complex behavior featured by the ESR spectrum below 18 K, mentioned earlier in this report, will be discussed in some detail in a future publication.

References

[1] DRESSELHAUS G. and DRESSELHAUS M. S., Intercalation in Layered Materials, M. S. Dresselhaus Ed., *NATO ASI Ser. B* **148** (1986).

[2] RANCOURT D. G., Chemical Physics of Intercalation, A. P. Legrand and S. Flandrois Eds., *NATO ASI Ser. B* **172** (1987).

[3] IKEDA H., SUZUKI M., MATSUURA M., SUEMATSU H., NISHITANI R., YOSHIZAKI R. and ENDOH Y., Graphite Intercalation compounds, S. Tanuma and H. Kamimura Eds., Summary Report of Special Distinguished Research Project « The study of Graphite Intercalation compounds » (March 1984) Japan, pp. 76-90.

[4] RANCOURT D. G., HUN B. and FLANDROIS S., *Ann. Phys. Fr.* **11** (1986) C2-107 ;
BARON F., FLANDROIS S., HAUW C. and GAULTIER J., *Solid State Commun.* **42** (1982) 759 ;
FLANDROIS S., MASSON J. M., ROUILLON J. C., HAUW C. and GAULTIER J., *Synth. Met.* **3** (1981) 1 ;
FLANDROIS S., HEWAT A. W., HAUW C. and BRAGG R. H., *Synth. Met.* 7 (1983) 305.

[5] ELAHY M., DRESSELHAUS G., *Phys. Rev. B* **30** (1984) 7225 ;
CHEN S. T., SZETO K. Y., ELAHY M., DRESSELHAUS G., *J. Chim. Phys.* **81** (1984) 863 ;
SUZUKI M., WIESLER D. G., CHOW P. C. and ZABEL H., *J. Magn. Magn. Mater.* **54-57** (1986) 1275 ;
SUZUKI M., WIESLER D. G., CHOW P. C. and ZABEL H., *Phys. Rev. B* **34** (1986) 7951 :
NICHOLLS J. T., SPECK J. S. and DRESSELHAUS G., *Phys. Rev. B* **39** (1989) 10047 ;
YEH N.-C., SUGIHARA K. and DRESSELHAUS M. S., *Phys. Rev. B* **40** (1989) 622 ;
ELAHY M., DRESSELHAUS G., NICOLINI C. and ZIMMERMAN G. O., *Solid State Commun.* **41** (1982) 289 ;
SZETO K. Y., CHEN S. T. and DRESSELHAUS G., *Phys. Rev. B* **33** (1986) 3453.

[6] NICHOLLS J. T. and DRESSELHAUS G., Intercalation in Layered Materials, M. S. Dresselhaus Ed., *NATO ASI Ser. B* **148** (1986) ;
RANCOURT D. G., *J. Magn. Magn. Mater.* **51** (1985) 133 ;
SZETO K. Y., CHEN S. T. and DRESSELHAUS G., *Phys. Rev. B* **32** (1985) 4628.

[7] WIESLER D. G., ZABEL H. and SUZUKI M., *Synth. Met.* **23** (1988) 237 ; *Phys. Rev. B* **36** (1987) 7051.

[8] HEROLD A., Chemical Physics of Intercalation, A. P. Legrand and S. Flandrois Eds., *NATO ASI Ser. B* **172** (1987) ;
HEROLD A., FURDIN G., GUÉRARD D., HACHIM L., NADI N. E. and VANGELISTI R., *Ann. Phys. Fr.* **11** (1986) C2-3 ;
SUZUKI M., OGURO I. and JINZAKI Y., Extended Abstracts GIC, Materials Research Society, Nov. 28-30, 1984 Boston, P. C. Eklund, G. Dresselhaus and M. S. Dresselhaus Eds., p. 91 ;
RANCOURT D. G., HUN B. and FLANDROIS S., *Can. J. Phys.* **66** (1988) 776.

[9] KUHLOW B., *Phys. Status Solidi (a)* **72** (1982) 161 ;
NARATH A. and DAVIS L., *Phys. Rev.* **137** (1965) A 163.

[10] LINES M. E., *Phys. Rev.* **131** (1963) 546.

[11] VANGELISTI R., HEROLD A., *Carbon* **14** (1976) 333.

[12] HAGIWARA M., KANABOSHI A., FLANDROIS S. and MATSUURA M., to be published (1990).

[13] BIENSAN P., FLANDROIS S., CHEHAB S. and AMIELL J., International Carbon Conference, 16-20 July 1990, Paris.

[14] BIENSAN P., Ph. D. Thesis, University of Bordeaux, France (1991).

[15] SUZUKI M., MURATA M. and SUEMATSU H., *Synth. Met.* **6** (1983) 173.

[16] SUZUKI M., KOGA K. and JINZAKI Y., Technical Report of ISSP, Series A, No. **1392,** published by « The Institute for Solid State Physics » The University of Tokyo, Japan (December 1983).

[17] SUZUKI M., KOGA K. and JINZAKI Y., Graphite Intercalation compounds, S. Tanuma and H. Kamimura Eds. ; Summary Report of Special Distinguished Research Project « The study of Graphite Intercalation compounds » (March 1984) Japan, pp. 98-110.

[18] GONZALEZ O., FLANDROIS S., MAAROUFI A. and AMIELL J., *Solid State Commun.* **51** (1984) 499.

[19] KOGA K. and SUZUKI M., *J. Phys. Soc. Jpn* **53** (1984) 786.

[20] FLANDROIS S., AMIELL J. and MASSON J.-M., *Phys. Lett.* **80A** (1980) 328.

[21] NISHITANI R., OHMATSU K., SUEMATSU H. and MURATA M., *Synth. Met.* **6** (1983) 185.

[22] YAMADA I. and IKEBE M., *J. Phys. Soc. Jpn* **33** (1972) 1334 ;
YAMADA I., MORISHITA I. and TOKUYAMA T., *Physica* **115B** (1983) 179.

[23] RICHARDS P. M. and SALAMON M. B., *Phys. Rev. B* **9** (1974) 32.

[24] RICHARDS P. M., Proceeding of the International School of Physics, « Enrico Fermi » Course LIX, North-Holland Amsterdam (1976).

[25] EGOROV G. A. and YABLOKOV Yu V., *Zh. Eksper. Teor. Fiz.* **39** (1960) 265.

[26] BROWN J., *J. Phys. Chem. USA* **67** (1963) 2524.

[27] HUBER D. L. and SEEHRA M. S., *J. Phys. Chem. Solids* **36** (1975) 723.

[28] DORMANN V. and JACCARINO V., *Phys. Lett.* **48A** (1974) 81.

[29] BIRGENEAU R. J., RUPP L. W. Jr., GUGGENHEIM H. J., LINDGARD P. A. and HUBER D. L., *Phys. Rev. Lett.* **30** (1973) 1252 ;
LOZENKO A. F. and RYABCHENKO S. M., *Sov. Phys. Solid State* **12** (1970) 624.

[30] YAMADA I., NAGANO S. and SHIMODA S., *Physica* **123B** (1983) 47.

[31] NAGATA K., YAMAMOTO I., TAKANO H. and YOKOZAWA Y., *J. Phys. Soc. Jpn* **43** (1977) 857.
[32] HUBER D. L. and SEEHRA M. S., *Phys. Status Solidi* (*b*) **74** (1976) 145.
[33] LINDGARD P. A., BIRGENEAU R. J., ALS-NIELSEN J. and GUGGENHEIM H. J., *J. Phys. C : Solid State Phys.* **8** (1975) 1059.
[34] VAKNIN *et al.* (*Phys. Rev. B* **35** (1987) 6423) have extended Richards and Salamon's theory (Ref. [23]) to the more general case of anisotropic exchange interaction.